Phys. Status Solidi C **13**, No. 10–12, 833–841 (2016) / **DOI** 10.1002/pssc.201600067

physica status solidi c
www.pss-c.com
current topics in solid state physics

Infrared defect dynamics – radiation induced complexes in silicon crystals grown by various techniques

Naohisa Inoue[*,1,6], **Takahide Sugiyama**[**,2], **Yasunori Goto**[***,3], **Kaori Watanabe**[****,4], **Hirofumi Seki**[*****,5], **and Yuichi Kawamura**[******,6]

[1] Tokyo University of Agriculture and Technology, 2-24-16, Nakacho, Koganei, Tokyo 187-8588, Japan
[2] Toyota Central Research Laboratories Inc., 41-1, Yokomichi, Nagakute, Aichi 480-1192, Japan
[3] Toyota Motor Corporation, 543, Kirigahora, Nishihirose, Toyota, Aichi 470-0309, Japan
[4] Systems Engineering Inc., 2-29-24, Honkomagome, Bunkyo-ku, Tokyo 113-0021, Japan
[5] Toray Research Center Inc., 3-3-7, Sonoyama, Otsu, Shiga 520-8567, Japan
[6] Osaka Prefecture University, 1-2, Gakuencho, Naka-ku, Sakai, Osaka 599-8570, Japan

Received 23 May 2016, revised 6 October 2016, accepted 26 October 2016
Published online 14 November 2016

Keywords infrared absorption, irradiation, point defects, silicon, power device

* Corresponding author: e-mail inouen@riast.osakafu-u.ac.jp, Phone: +81 424-64-0853, Fax: +81 424 64 0853
** e-mail t-sugiyama@mosk.tytlabs.co.jp, Phone: +81 561 63 4724, Fax: +81 561 63 6042
*** e-mail yasunori_goto@mail.toyota.co.jp, Phone: +81 565 46 3358, Fax: +81 565 46 3382
**** e-mail watanabe@systems-eng.co.jp, Phone: +81 3 3946 4993, Fax: +81 3 3946 4983
***** e-mail Hirofumi_Seki@trc.toray.co.jp, Phone: +81 77 533 8609, Fax: +81 77 533 8696
****** e-mail kwmr@riast.osakafu-u.ac.jp, Phone: +81 72 254 9832, Fax: +81 72 254 9935

Radiation induced point defect-light element impurity complexes, basically C_iO_i, are used widely for lifetime control in power devices for hybrid cars. Recently, not only CZ, but also FZ and epitaxial wafers have been examined as candidates. It has been suggested by luminescence study that C_iO_i behaved differently during annealing in crystals from different origins. The behavior of C_iO_i (and VO) during annealing was examined by highly sensitive infrared absorption spectroscopy (IR). C_iO_i concentration ($[C_iO_i]$) after irradiation depended strongly on the growth techniques and as-grown carbon ([C]) and oxygen ([O]) concentrations. In the basic C-rich MCZ case, C_iO_i and VO reacted with each other and decreased steadily with annealing temperature increase. They mostly disappeared at 400 °C. In low [C] CZ case, C_iO_i residual ratio (RR = $\alpha_{400°C}/\alpha_{RT}$, α is the absorption coefficient) was higher, probably due to low reaction probability of much lower $[C_iO_i]$ with VO. In FZ silicon, C_iO_i residual ratio was low, probably due to rapid break. Thus, IR made systematic and quantitative analysis compared to the luminescence study. In nitrogen-doped FZ silicon, NV was observed in as-grown crystals. N_2 was modified by irradiation and complicated reaction took place with V or I by annealing. This would affect the C_iO_i behavior.

1 Introduction Silicon crystals have been used mainly for LSIs. Recently, power devices, especially those for hybrid cars, have become important application [1]. Today, radiation induced complexes C_iO_i are used widely for improving performance of inverters for mobile cars [1]. The behavior of radiation induced light element impurity-intrinsic point defect complexes such as C_iO_i has long been analyzed, mainly on high carbon concentration ([C]) samples under high dose irradiation [2]. It, however, has become practically important to understand the behavior in high quality low [C] substrates under low dose irradiation. In addition, CZ silicon was the main substrate to date, but FZ and epitaxial silicon are also the candidates for power device substrates now. The behavior of C_iO_i and the effect on device performance has usually been analyzed by photoluminescence (PL) and cathodoluminescence (CL) or deep level transient spectroscopy (DLTS) [1]. Since these methods can detect only a fraction of these complexes, we have used infrared absorption measurements which can detect almost all complexes and is quantitatively reliable. We

have, in fact, established highly sensitive, quantitative and systematic infrared absorption spectroscopy and used the analysis on defect dynamics from 2006 [3] (we called this method "infrared defect dynamics" [4]). Here, the behavior of C_iO_i with emphasis on that of related complexes such as VO and in various crystals was examined in detail. These results are compared with those arising from PL and CL measurements.

2 Experimental We examined various middle [C] MCZ (magnetic CZ) [4] and low [C] CZ [5] silicon, FZ silicon [6] and NCZ (nitrogen doped) silicon [6]. Sample size was about 1 cm square and 2 mm thick with both sides mirror polished. Impurity concentrations, [C] and [O] (oxygen) and conductivity type and dopant are summarized in Table 1. [C] and [O] were obtained from the absorption coefficient (α) by using the conversion coefficients 0.82 and 3.14 x 10^{17} atoms/cm^2 given in SEMI MF1391 and MF1188, respectively.

The samples were irradiated by electrons accelerated at 4.6, 2 or 1 MeV (in the last case from both sides) at room temperature. He irradiation was done on middle [C] MCZ crystal at an acceleration voltage of 5 MeV [7]. After irradiation, the samples were annealed at from 100 to 800 °C (temperature range was different for different sample sets) separately for each temperature for 10 min.

Differential infrared absorption measurement of the irradiated and annealed samples was done using non-irradiated sample as the reference at room temperature. The wavenumber resolution was 2 cm^{-1} or 4 cm^{-1} (the latter was used for ultra low concentration complexes). The noise level was about 10^{-7} absorbance at best and the complex absorption lines with 10^{-6} peak height were successfully detected and evaluated [7]. To improve the reliability, a few absorption lines from the same complex were measured and compared (complexes and absorption lines are listed in the Appendix).

Table 1 [C], [O] (cm^{-3}), α_{CiOi} (862 cm^{-1}), α_{VO} (830 cm^{-1}) and residual ratio (RR) in various crystals.

	[C]	[O]	$A_{As\ ir.}$		$\alpha_{400°C}$		$RR_{(400/RT)}$		type
	E15	E17	CiOi	VO	CiOi	VO	CiOi	VO	
C-rich	9	2.5	0.0197	0.0273	0.0025	0	0.15	0	N(As)
C-med	1.5	9	0.0028	0.1035	0.0014	0.0023	0.50	0.02	P(B)
FZ	0.4	0.2	0.0059	0.0434	0	0	0	0	P(B)
NCZ	1	7	0.0013	0.1150	0.00049	0.00024	0.39	0.002	P(B)

3 Results and discussion

3.1 Middle [C] MCZ crystal In this case, [C] = 9 x 10^{15} and [O] = 2.5 x 10^{17} cm^{-3}. Figure 1(a) shows the differential absorption spectra of so called C-rich [2] case. The spectra for the annealing temperature between 300 and 400 °C are shown here and those for as irradiated and annealing at 100 and 200 °C had been shown in Ref. [8], Fig. 5. There are more than 10 complexes and more than 20 absorption lines: $-C_s$ (**605** cm^{-1}), $-O_i$ (515, **1107**), C_iO_i (545, 738, **862**, 1109), IC_i (956, **962**), IC_iO_i (**936**, 1020), IC_iO_i** (947, **966**), $I_2C_iO_i$ (**994**), $I_3C_iO_i$ (**990**), C_sO (585, **635**, 685, 1096, 1104), C_sO_2 (**1048**, 1094), VO (**830**), VO_2 (**888**), VO_2* (**923**), V_2O(833), V_3O (839) and #1020 (unidentified yet, at 1020 cm^{-1}). Assignment mostly followed that by Murin et al. and Lindstroem et al. The bold wavenumber lines are mainly used for quantitative discussion. The reactions including C_iO_i and its counterpart VO at above 350 °C were suggested to be simple. They are expressed by the following three equations and indicated by arrows in Fig. 1(a) [2]:

$$C_iO_i + VO \rightarrow C_sO + O\,, \quad (1)$$

$$VO + O \rightarrow VO_2\,, \quad (2)$$

$$C_i + VO_2 \rightarrow C_sO_2\,. \quad (3)$$

In detail, (1) includes pre-reactions $C_iO_i \rightarrow C_i+O_i$ or $VO \rightarrow V+O$, both emit excess O, before meet with each other. The last one (3) was usually observed only in the irradiation at elevated temperature [9, 10]. In this case, however, both C_sO and C_sO_2 were observed by irradiation at RT as marked in Fig. 1(a) and shown in more detail in Fig. 1(b) (CsO_2 at 1048 and 1094 cm^{-1}). VO has two parallel reactions competing with each other, as shown in Eqs. (1) and (2). Product VO_2 of reaction (2) was removed by the reaction (3). As already reported, the other complexes, minor ones, were much less and did not react with the major complexes described here, need not to be taken care of [4]. Figure 2(a) shows the annealing temperature dependence of the peak absorbance of major complexes. Both [C_iO_i] and [VO] started to reduce at 350 °C and most of them disappeared at 400 °C. Instead, C_sO, C_sO_2 and VO_2 monotonously increased from 350 to 400 °C. The presence of C_iO_i upto 400 °C was confirmed by the 1109 cm^{-1} line shown in Fig. 1(b). Different signals from the same origin improved the reliability. Figure 2(b) shows the various signals from C_iO_i. Good agreement between the temperature dependence of 862 and 1109 cm^{-1} lines was confirmed. Unfortunately weaker signals of 545 and 738 cm^{-1} lines and CL intensities were not reliable quantitatively. At 400 °C, the absorption at around 830 cm^{-1} had not a sharp line. The magnified picture is shown in Fig. 1(c). There were five apparent peaks at about 823, 829, 831, 834 and 840 cm^{-1}. They were similar to the 826 (VO_2), 834, 839 (V_3O) cm^{-1} bands [11], 833.4 cm^{-1} (V_2O) bands (LT) [12] and 825 (V_2O_2), 834 (V_3O_2) and 840 (V_2O) cm^{-1} (1 cm^{-1} shifted upward from the original paper according to that VO=829 (830 is correct) and VO_2=887 cm^{-1} (888 is correct) in the paper) bands [13]. Among them, the 829 and 840 cm^{-1} bands were strong here, but the VO 830 cm^{-1} line was hardly observed. Unfortunately there was the interference fringe which prevented us to get correct peak wavenumber. Quantitatively, the absorption coefficients (α) are summarized in Table 1. Because the conversion coefficient (k) to concentrations

was $k_{VO} = 3\ k_{CiOi}$ (see the dipoles in the table of the Appendix), [VO] was more than 4 times higher than [C_iO_i]. As a result, both were enough to react with and most were consumed. Only about 15% (residual ratio, RR = $\alpha_{400\ oC}/\alpha_{RT}$) of C_iO_i left after the annealing at 400 °C. Loss of VO was much higher, transformed into VO_2, V_2O, V_3O and so on. The peak height of C_sO and C_sO_2 of the sample annealed at 400 °C was much lower than that of initial C_iO_i. This suggested that the dipole of C_sO and C_sO_2 (assumed to be almost equal with each other) was much smaller than that of C_iO_i. There is the discussion on C_iO_{i2} or P-line [14, 15]. We have not enough information to discuss this now. The annealing time was 10 min. in this case and the P-line had been shown to develop up to 100 min.

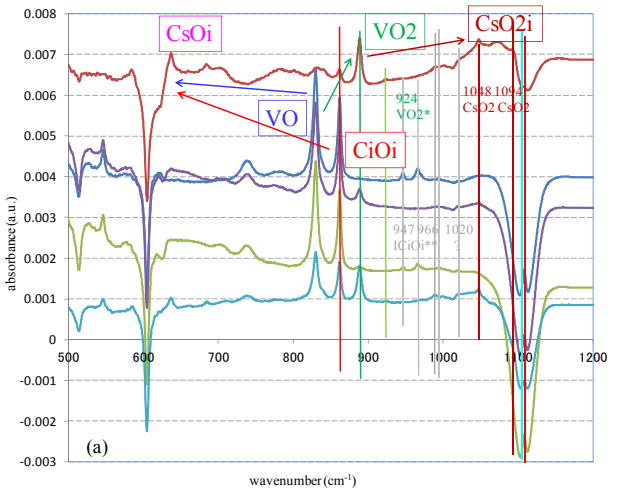

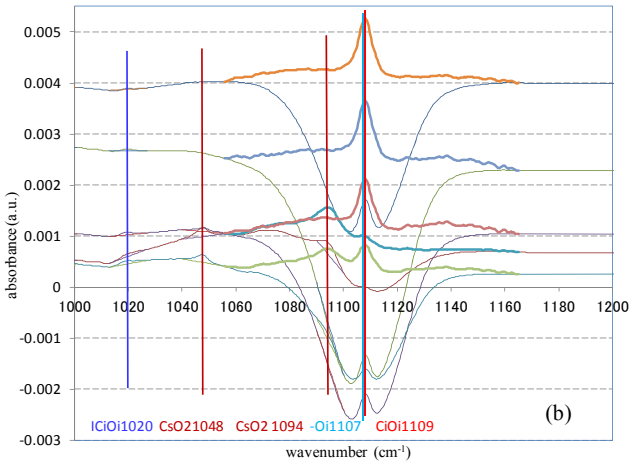

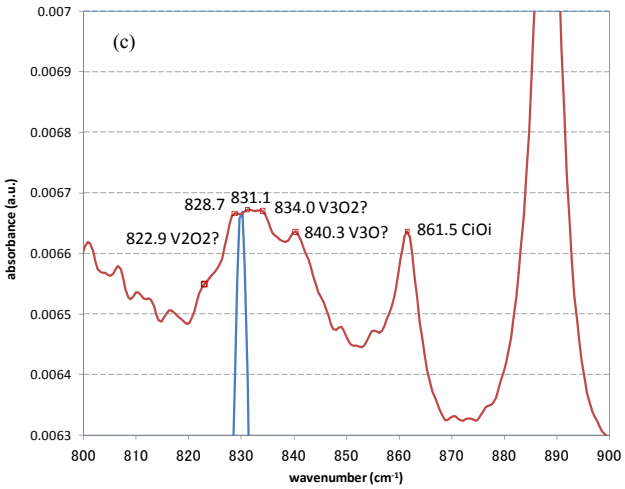

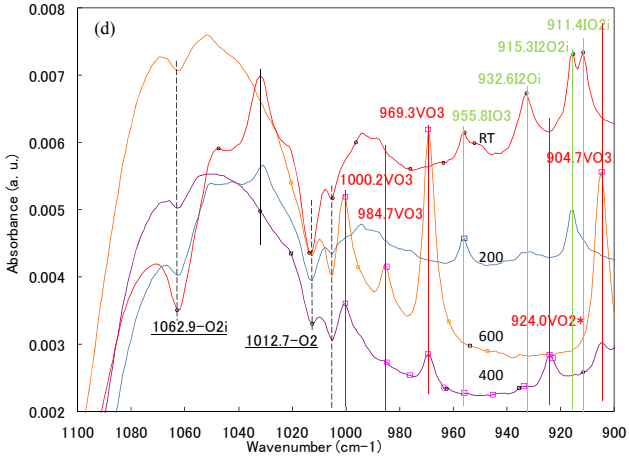

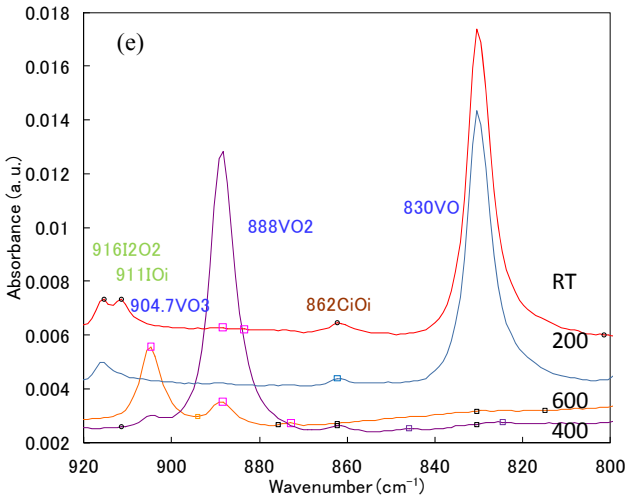

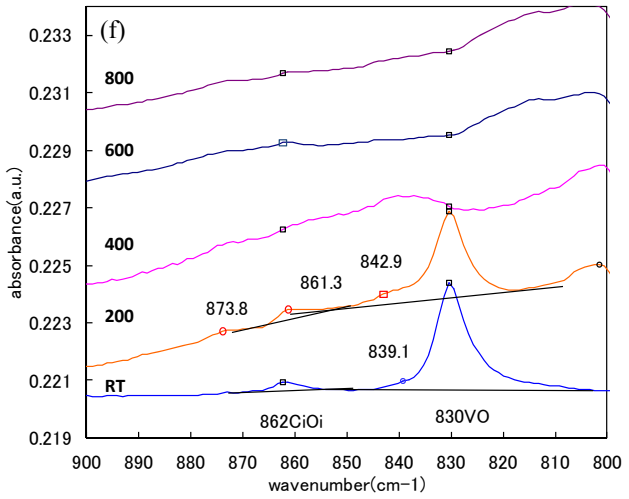

Figure 1 Annealing temperature dependence of differential absorption spectra of irradiated and annealed silicon. (a) C-rich MCZ, after annealing at 300, 325, 350, 375 and 400 °C. Absorption lines are labelled and the dominant reactions are indicated. (b) Ibid, C_sO_2 absorption at 1048 and 1094 cm^{-1} and C_iO_i absorption (delineated by cancelling the O_i loss) at 1109 cm^{-1}. (c) Ibid, magnified spectra at around 830 cm^{-1} for 400 °C. (d) Low [C] CZ, between 900 and 1100 cm^{-1}. (e) Ibid, magnified spectra between 800 and 920 cm^{-1}. (f) FZ, magnified spectra between 800 and 900 cm^{-1}. Vertical unit is absorbance A. Absorption coefficient is α = A x 11.3 (= (log10/loge) x (1 cm/2 mm)).

3.2 low [C] CZ silicon Carbon concentration in commercial silicon has been decreasing recently. Low [C] samples were examined here. The most examined sample contained [C] = 1.5 x 10^{15} and [O] = 8.6 x 10^{17} cm^{-3} [6]. Previously, low [C] samples have been categorized C-lean type in the irradiation studies [10]. In the C-lean case, C-rich type complexes listed above including C_iO_i have not been observed but C-lean type IO_{2i} group was observed, IO_{2i} (**911** cm^{-1}), I_2O_{2i} (**916**, 1031), IO_{3i} (**956**) , O_{2i} (**1013**, 1062) and TDD (thermal double donor, 976, 989, 999, 1006 cm^{-1}) [8]. Here, however, C_iO_i group was observed in addition to IO_{2i} group, owing to the ultra high sensitivity. Therefore we call this case "C-medium." An example of the spectra between 800 and 1100 cm^{-1} (as irradiated and after annealed at 200, 400 and 600 °C) is shown in Figs. 1(d) and (e). 862 cm^{-1} absorption line due to C_iO_i was much weaker than the 830 cm^{-1} VO line due to low [C]. C_iO_i absorption was clearly observed after annealing at 200 and 400 °C, in contrast to the C-rich case described above. VO absorption at 830 cm^{-1} was almost disappeared at 400 °C as in the C-rich case. Figure 2(c) shows the annealing temperature dependence of the peak absorbance. α_{CiOi} was15% and α_{VO} was 1/4 of the above C-rich case, respectively. After annealing at 400 °C, α_{CiOi} was 1/2 (=RR) of that after irradiation. The reaction was basically same as that in the C-rich case. It is considered, however that, as [C_iO_i] was very low, less than 15% of C-rich case and 3% of [VO], the reaction probability with VO was much reduced, resulting in more part of C_iO_i left after annealing at 400 °C (RR=1/2). On the other hand, almost all VO changed into VO_2, due to rich [O] and that the reaction (2) of VO with O was superior to that (1) with C_iO_i. At above 400 °C, VO_n (n > 2) were formed. We do not discuss VO_n (n ≥ 3) here (they had been discussed in detail in [16]. The effect of presence of IO_{2i} group will be examined in the future.

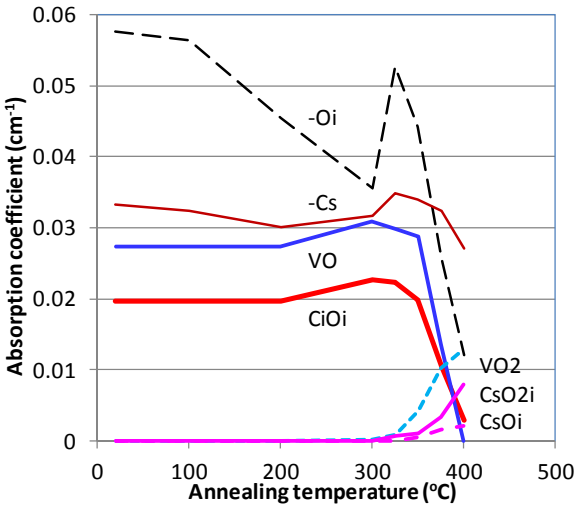

(a)

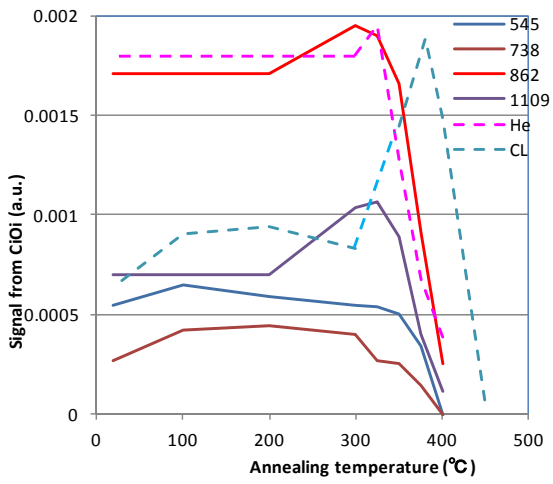

(b)

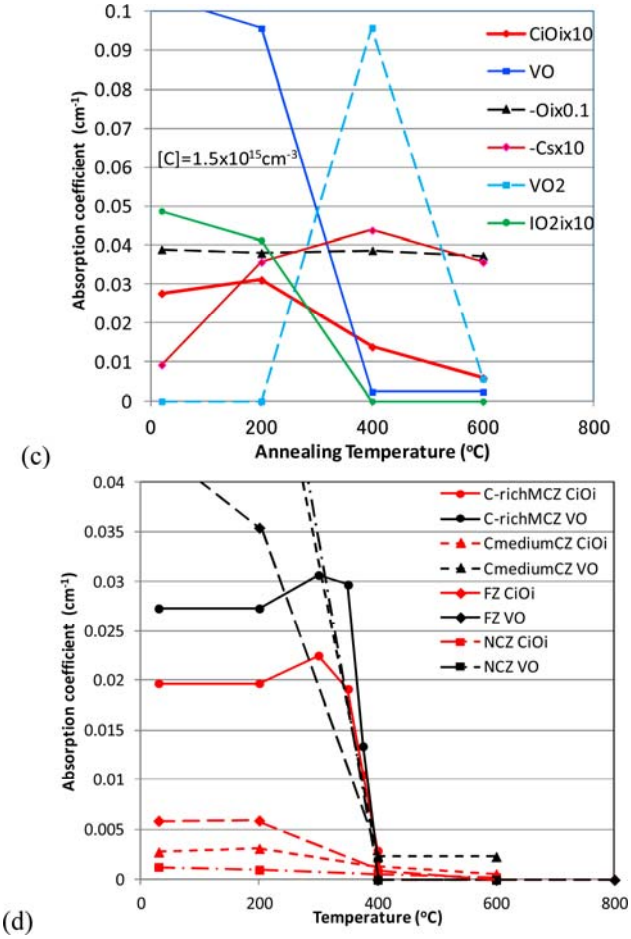

Figure 2 Annealing temperature dependence of peak absorbance of dominant complexes including C_iO_i and VO. (a) C-rich MCZ case. (b) Ibid, various signals from CiOi, (c) C-medium CZ case. Someones are magnified or reduced. (d) Summary of C_iO_i and VO including FZ and NCZ cases.

3.3 FZ silicon crystal FZ crystals, not using crucible, contain more than 1 order of magnitude less [O] than CZ crystals which use SiO_2 crucible. Dependence of the spectra on sample and annealing temperature had been shown in [6] Figs. 1 and 2. One example of behavior is discussed in detail here. [C] was about 1 x 10^{15} cm^{-3} and [O] about 2 x 10^{16} cm^{-3}. As shown already in [6] Fig. 1, C-rich type C_iO_i absorption lines, at 545, 862 and 1109 cm^{-1}, IC_iO_i at 936 and 1020 cm^{-1}, $I_2C_iO_i$ and $I_3C_iO_i$ at 994 and 989 cm^{-1}, and VO line at 830 cm^{-1} were observed though [O] was low, but C-lean type complexes were not observed after irradiation. This was similar to the C-rich MCZ case described above. Annealing temperature dependence of the spectra between 800 and 900 cm^{-1} is shown in Fig. 1(f). C_iO_i and VO were observed after irradiation and annealing at 200 °C, but not after annealing at 400 °C. This resembled to middle [C] CZ case. The difference was that C_iO_i and VO decreased a little after annealing at 200 °C. Also, VO_n ($n \geq 2$) was not formed by annealing at above 400 °C These were not observed in CZ silicon. At 400 °C C_sO_2 (1048 and 1094 cm^{-1} lines) was not confirmed. Figure 2(d) shows the temperature dependence of the absorbance. After irradiation α_{CiOi} was 2 times larger and α_{VO} was less than 1/2 of C-medium crystal but 7 times higher than α_{CiOi}. C_iO_i content and thermal behavior was similar to that in C-medium CZ crystal. Here, VO content reduced rapidly with temperature by VO → V+O due to low [O]. As [C_iO_i] was low and VO was rapidly broken, they did not meet easily with each other. C_iO_i was considered to be broken.

3.4 Nitrogen doped crystal Nitrogen doping in silicon crystal is widely used to suppress grown-in microdefects [17]. The interaction between N and intrinsic point defects of both I and V plays an important role in the defect formation. It also should affect the C_iO_i behavior in power devices using N-doped silicon crystal. Both CZ and FZ crystals were examined. Nitrogen concentration ranged 2 x 10^{14}-6 x 10^{15} cm^{-3}. The result of an example of NCZ case is shown in Table 1 and Fig. 2(d). [C] and [C_iO_i] were about 1/10 of C-rich MCZ case and 1/2 of C-medium CZ case. The behaviour was similar to C-medium CZ case and the residual ratio (RR) was also high, 0.39. This will be examined in more detail in the future.

N_2 absorption line apparently weakened by the irradiation of FZ crystal. On the other hand, the reduction was not observed in CZ crystal. New peaks appeared at 778, 725, and 551 (NV) cm^{-1} in FZ Si as shown in Fig. 3(a). NV band at 551 cm^{-1} had been observed only in laser annealed and quenched sample [18]. The linear relation of loss of 766 and gain of 778 cm^{-1} lines suggested that the latter's origin was some transform from N_2. By the post-annealing, N_2 absorption lines recovered and several new absorption lines appeared as shown in Fig. 3. Among them, those at 689 and 725 cm^{-1} were prominent. The intensity of the lines at 778 and 725 cm^{-1} reduced monotonously as the annealing temperature increased. The loss of N_2 absorption lines increased a little with higher annealing temperature and steeply increased by the annealing at 600 °C but almost disappeared at 800 °C. The absorption lines at 778, 725 and 551 (not shown here) cm^{-1} weakened monotonously upto 400 °C and disappeared at 800 °C. The absorption line at 689 cm^{-1} appeared by the annealing at 400 °C and with smaller intensity at 600 °C, but not appeared at 800 °C.

From the behavior of the 766 and 778 cm^{-1} lines, it is plausible that N_2 was not completely destroyed but something was added by the irradiation. The accompanying complexes were C-rich type only and C-lean (I-rich) types were not found. This suggested the V-rich condition and the added material was thought to be V rather than I. Jones [19] calculated and examined the N_iN_s (VN_2) to be at 774 cm^{-1} and related it to the 782 and 790 cm^{-1} lines from unknown structure observed by Goss [20]. Here, we tentatively assigned 778 (and 726) cm^{-1} lines to VN_2. Karoui [21] calculated VN_2 also and obtained 781 and 585 cm^{-1}

lines, and related 585 cm^{-1} to observed 551 cm^{-1} and assigned to N_s by Stein.

On annealing at 400 °C, 689 and 724 cm^{-1} lines appeared instead of 778 and 725 cm^{-1} lines. Simple explanation was further attachment of V resulting in the formation of V_2N_2. VO disappeared on annealing at 400 °C. In contrast, in CZ silicon VO transformed into VO_2. These suggested that VO released both V and O in FZ silicon here as described above. Karoui [21] calculated V_2N_2 absorption, to be at 615, 625 and 637 cm^{-1}, and related to the observed 653 cm^{-1} line by Stein (N_s). We tentatively assigned 689 (and 714) cm^{-1} lines to be from V_2N_2. The stability of VN_2 and V_2N_2 had been theoretically examined in relation to the effect of nitrogen on the grown-in defect formation in Si. The above results made it possible to estimate the dipole of VN_2 (2/3 of N_2) and V_2N_2. N changes both [V] and [I]. These N-V interactions might affect the C_iO_i behavior in NFZ silicon.

3.5 He irradiation He irradiation is used to introduce C_iO_i to the power devices for the hybrid cars [1]. It was examined here on the samples from the same C-rich MCZ crystal as that used in the electron irradiation described in Section 3.1 [7]. Absorption lines were mostly similar to those shown in Section 3.1. Not only C-rich type complexes such as C_iO_i and IC_iO_i, however, but also C-lean type complexes such as I_2O_{2i} and IO_{3i} shown in Section 3.2 (C-medium CZ case) were observed, in contrast to the electron case. Peak absorbance for He case is about half that of electron irradiation. He dose was 5 x 10^{13} cm^{-2}, 1/200 of the electron dose of 10^{16} cm^{-2}. Peak absorbance A corresponds to the total amount of complexes in the sample. In this case $A_{He} = 1/2A_{El}$. As for the dose $F_{He} = 1/200A_{El}$. Production rate (P) = A/F. $P_{He}/P_{El} = (1/2/1/200)/1/1 = 100$. Thus, the complex production rate per particle was about 100 times as large as that of electron. The production range in He case was restricted to 20 μm from the surface, 1/100 thickness of the electron case in which complexes had been formed uniformly throughout the 2 mm thick sample. Therefore, the complex concentration in the layer was about 100 times as high as that in the electron case. Annealing behavior of C_iO_i and others was similar to that in the electron case, but there was some difference in the detail. The annealing temperature dependence of C_iO_i peak intensity is compared to the electron case in Figs. 2(b) and (d). Electronic property of IO_{2i} was examined [22]. This must be taken into account for low [C] crystals.

3.6 Comparison to PL studies These studies were mainly addressed at the analysis of the dependence of C_iO_i on the crystal type by photoluminescence (PL) for power device application [23, 24]. The temperature dependence of normalized luminescence (C-line) from C_iO_i was examined. In case of FZ crystals, annealing out temperature was about 350, 375 and 450 °C for the specimen with [C] 9, 8, 3x10^{14} and [O] 1, 2x10^{15} and 1 x 10^{17} (CZ-FZ) cm^{-3}, respectively. The authors of the papers suggest that the high [O] kept the anneal temperature high. In their other study including CZ crystal, C_iO_i anneal temperature was 350 for gas-dope FZ, 375 for poly-FZ, 400 for CZ-FZ and 450 °C for MCZ (carbon ND and [O] highest). They considered that the unbalance of [C]/[O] reduced the bonding probability with each other. In the other DLTS study, deep level due to VO had been observed differently in the different FZ crystals and had been suggested to be responsible for diode characteristic difference [25]. In our study, however, Goto et al. observed VO also in the He irradiated diodes, but did not find correlation to the device characteristic difference [26]. Sugiyama et al. did cathodoluminescence (CL) study after He irradiation. As shown already in Ref. [7] and in Fig. 2(d), the luminescence intensity was modified from the [CiOi] and restricted usually only to C_iO_i. IR gives a quantitative information of all related complexes as shown here. A difference of VO behavior in FZ from that in low [C] CZ, for example, was found. Thus, "infrared defect dynamics" will help to clarify the behavior and mechanism.

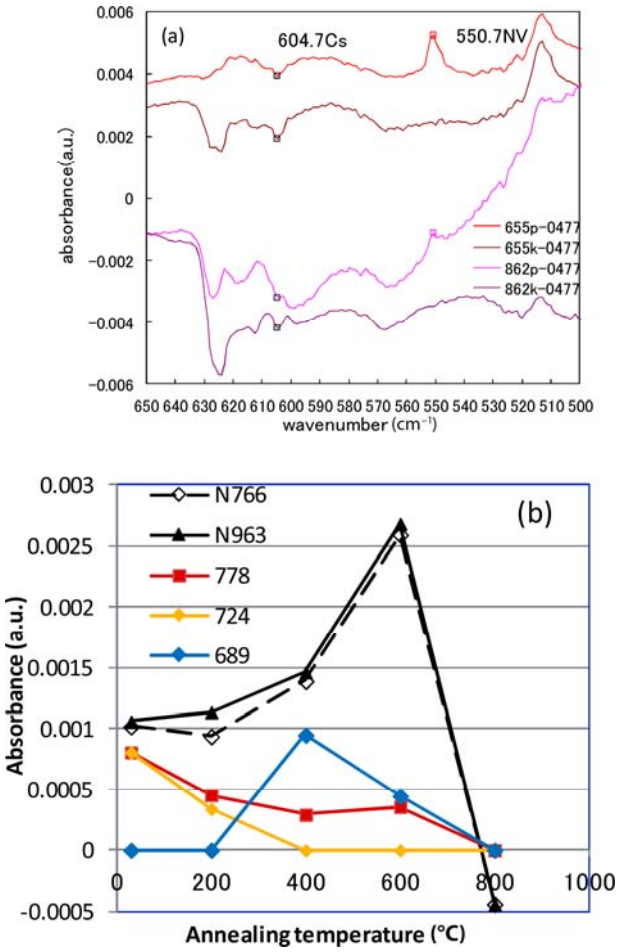

Figure 3 (a) NV band at 551 cm^{-1} observed in as-grown NFZ silicon. (b) Annealing temperature dependence of loss of absorption from N_2 and new absorption in irradiated NFZ silicon.

4 Summary In summary, behavior of radiation induced C_iO_i (and VO) during post annealing in crystals grown by various techniques was examined by highly sensitive and systematic infrared absorption spectroscopy. Not only dominant complexes but also minor groups were analyzed for the first time. Carbon concentration ([C]) ranged 5 x 10^{14}-1 x 10^{16} and oxygen concentration ([O]) between 1 x 10^{16} and 5 x 10^{17} cm^{-3}. In the most well established C-rich type middle [C] MCZ silicon, C_iO_i and VO were dominant and almost disappeared by the annealing at 400 °C. At above 300 °C they reacted with each other as C_iO_i+VO=C_sO+O. They steadily decreased with annealing temperature up to 400 °C where most C_iO_i and all VO were consumed. VO+O=VO_2 also took place and competed with the above reaction. From VO_2, C_i+VO_2=C_sO_2 also took place. It is to be noted that the complexes in C_iO_i-VO-C_sO system react only within this system. In the other crystals, low [C] CZ and FZ silicon, C_iO_i was minor. In a new "C-medium" type, [C_iO_i] was comparable to [IO_{2i}] group which are known to be dominant in C-lean type crystals. For low [C] CZ silicon, higher ratio of C_iO_i was reserved. It was probably due to that low content C_iO_i after irradiation could not easily react with VO. In low [O] FZ silicon, such residual C_iO_i was not confirmed yet, probably due to that they were rapidly broken. In the luminescence studies C_iO_i residual ratio by C-line intensity at 400 °C had been reported to be higher in MCZ and FZ silicon than in CZ silicon. It was difficult whether [C_iO_i] was high or nonradiative center concentration was low. Moreover it could not reveal the behaviour of source and product of C_iO_i. Highly sensitive and quantitative IR study will reveal the behaviour. In nitrogen-doped FZ silicon, N_2 was modified by irradiation and complicated reaction took place with V or I. This would affect the C_iO_i behavior. The case of He irradiation was similar to that of electron irradiation.

Acknowledgements The authors are grateful to H. Ono (Kanagawa IRI) and K. Hoshikawa (Shinshu U.) for sample crystals, H. Hanaya (JAEA) for irradiation and L. I. Murin (ISSSP, Belarus), B. G. Svensson (U. Oslo), V. P. Markevich (U. Manchester), C. A. Londos (U. Athens), R. Jones (U. Exeter), H. Y. Kaneta (Kyushu I. Technol.), S. Saito (Renesas) and S. Okuda (Osaka Pref. U.) for discussion.

References

[1] T. Sugiyama, this Symposium, K11.2.
[2] L. I. Murin, V. P. Markevich, J. L. Lindstroem, M. Kleverman, J. Hermansson, T. Hallberg, and B. G. Svensson, Solid State Phenom. **82-84**, 57 (2002).
[3] N. Inoue, Y. Goto, T. Sugiyama, S. Yamazaki, and T. Kushida, High Purity Silicon IX, ECS Trans. **3**(4), 313 (2006).
[4] N. Inoue, Y. Goto, T. Sugiyama, H. Seki, K. Watanabe, and Y. Kawamura, Solid State Phenom. **205-206**, 228 (2014).
[5] N. Inoue, Y. Goto, T. Sugiyama, and Y. Kawamura, Phys. Status Solidi C **9**, 1931 (2012).
[6] N. Inoue, H. Oyama, K. Watanabe, H. Seki, and Y. Kawamura, Proc. 27th International Conference on Defects in Semiconductors, Bologna, Italy, 2013, pp. 19-23.
[7] N. Inoue, Y. Goto, T. Sugiyama, K. Watanabe, H. Seki, and Y. Kawamura, Phys. Status Solidi B **251**, 2205 (2014).
[8] N. Inoue, Y. Goto, and T. Sugiyama, Solid State Phenom. **131-133**, 207 (2008).
[9] L. I. Murin, V. P. Markevich, J. L. Lindstroem, M. Kleverman, J. Hermansson, T. Hallberg, and B. G. Svensson, Solid State Phenom. **82-84**, 57 (2002).
[10] J. L. Lindstroem, L. I. Murin, T. Hallberg, V. P. Markevich, B. G. Svensson, M. Kleverman, and J. Hermansson, Nucl. Instrum Methods Phys. Res. B **186**, 121 (2002).
[11] L. I. Murin, B. G. Svensson, J. L. Lindstroem, V. P. Markevich, and C. A. Londos, Solid State Phenom. **156-158**, 129 (2010).
[12] J. L. Lindstroem, T. Hallberg, J. Hermansson, L. I. Murin, V. P. Markevich, M. Kleverman, and B. G. Svensson, Solid State Phenom. **69-70**, 297 (1999).
[13] N. V. Sarlis, C. A. Londos, and L. G. Fytros, J. Appl. Phys. **81**, 1645 (1997).
[14] G. Davies, S. Hayama, L. Murin, R. Krause-Rehbeg, V. Bondarenko, A. Sengupta, C. Davia, and A. Karpenko, Phys. Rev. B **73**, 165202 (2006).
[15] B. Raeissi, N. Gonagona, A. Galeckas, E. V. Monakhov, and B. G. Svensson, Solid State Phenom. **205-206**, 224 (2014).
[16] L.I. Murin and J.L. Lindstroem et al., Solid State Phenom. **108-109**, 267 (2005).
[17] T. Abe, T. Masui, H. Harada, and J. Chikawa, Proc. 2nd Int. Symp. VLSI Sci. and Technol. (Electrochem. Soc., Pennington), p. 543 (1985), and others.
[18] H. J. Stein, Appl. Phys. Lett., 47, 1339 (1985).
[19] R. Jones, I. Hahn, J. P. Goss, P. R. Briddon, and S. Öberg, Solid State Phenom. **95-96**, 93 (2003).
[20] J. P. Goss, I. Hahn, R. Jones, P. R. Briddon, and S. Öberg, Phys. Rev. B **67**, 045206 (2003).
[21] F. S. Karoui and A. Karoui, Application of Quantum Mechanics for Computing, the Vibrational Spectra of Nitrogen Complexes in Silicon Nanomaterials, in: Some Applications of Quantum Mechanics, edited by M. R. Pahlavani (In Tech, 2012).
[22] V. P. Markevich, L. I. Murin, S. B. Lastovskii, I. F. Medvedeva, J. L. Lindstroem, A. R. Peaker, J. Coutinho, R. Jones, V. J. B. Torres, S, Oeberg, and P. R. Briddon, Solid State Phenom. **108-109**, 273 (2005).
[23] A. Kiyoi, M. Tanaka, T. Kawakami, H. Tsuruda, J. Tanimura, T. Minato, and M. Tarutani, Abstracts Japan. Soc. Appl. Phys., Spring Meeting, 19p-F9-14, Tokyo (2014) (in Japanse).
[24] T. Minato, K. Takano, and A. Kiyoi, JSPS #145 Commitee 145th Meeting (2017, Tokyo), p. 18 (in Japanese).
[25] S. Saito, private communication.
[26] Y. Goto, Proc. LSI Testing Symposium 2009 (LSI Testing Society 2009), p. 275 (in Japanese).
[27] M. Suezawa, Phys. Rev. B **63**, 35201 (2000).
[28] N. Fukata, T. Ohori, M. Suezawa, and H. Takahashi, J. Appl. Phys. **91**, 5831 (2002).

Appendix

Tentative list of infrared absorption lines from radiation induced light element impurities (C, O, N) - intrinsic point defects (vacancy V and self interstitial I) complexes. Complex, wavenumber of absorption line both at RT and at LT, normalized dipole (estimated conversion coefficient from absorption coefficient to concentration, that of carbon (SEMI MF1391: 0.82×10^{17} cm^{-2}) as 1. Complexes are grouped. The references were listed in references [3–7] here. The assignment follows mainly those by Murin and Lindstroem. For hydrogen see Ref. [27, 28].

common type:							dipole
Cs	**605**	1206					**1**
LT	607						
Oi	514	560	**1107**	1226			3.9
	515	1136					
VO	531	**830**	876				3.4
LT	534	835.8	885.5	1370			
VO−		877.1					
LT	545	885	1430.1				
formed by annealing:							
VO2	889						1.7
LT	895.5						
VO2*	923						
LT	928.4	1003.8					
V2O	826						
LT	833.4	1003.8					
V2O2	824						
LT	829	923	1000				
V3O2	833						
LT							
V3O	839						
LT	842.4						
VO3	905	969	**1000**	(985)			
LT							
LT	910	975.9–1005.3		1105	(991)		
VO3C	902	956	1025				
LT	985	1009					
VO4	985	1009					
LT	992	1011	1024	1041	1043	1056	1062
VO5,6LT	991	1011	1024	1040.6	1042.7	1056	1062
	1097	1097	1099	1108			
LT	842.4						
C-rich type:							
Ci	922	932					
LT							
CiOi	527	537	545	583	738	**862**	1109	1.2
LT	529.6	542	549.8	588	742.8	866	1116.3	
ICiOi	**936**	1020						1.2
LT	939.8	1024.2						
ICi	954	**962**						1.3
LT	960.1	966.7						
I2CiOi	**994**							3.4
LT	998							
I3CiOi	**988**							3.4
LT								
formed by annealing:								
CsO	585	**635**	685	1096	1104			
LT	589			1104	1104			2.4
CsO2	**1048**	1094						2.4
LT		1099.5						
ICiOi*	724.5	952.1	973.1					
ICiOi**	947	**966**						1
LT	951.3	969.3	977.8					
#1020	**1020**							1.2
C-lean type:								
I Oi								
LT	944.3	956.2						
IO2i	545	922	1042					
LT		922	1037					
I2O2i	916	933	1031					
LT	545	917	1034					
IO3i								
LT	956	1054						
I2Oi								
LT	936							
O2i	552	686	1013	1062				
LT	555.9	690.1	1012.4	1059.8	1105.3			
O3i								
LT		1006.8						
O-lean type:								
CiCs(G)								
LT	540.4	543.3	579.8	640.6	730.4			
CsCs								
LT	527.4	(748.7)						
TDD	578	730	975	988	999	1006	1013	
LT	580	730			1000			
Intrinsic point defect cluster:								
V2	1.8um							

LT	2767							
I3 (W)	62.7meV							
LT	565							
I4 (X)	66.2meV	67.9meV	69.0mV					
LT	534	548	557					
Nitrogen:								
N2	**766**	**963**						0.9
Ns(VN)	551	653						
VN2	725	**778**						0.9
V2N2	689	713						
Hydrogen:								
H LT								
VH	2067.5							
VH2	2122.4	2145.2						
VH3	2167	2191.8						
VH4	2222.9							
V2H2	2072.5							
IH2	1987.2	1990.1	743.1	748				
I2H2	1870.2							
H2*	1838.7	2062.1	817.6					
H2	3618.9							